Desalination and Water Treatment
www.deswater.com
doi: 10.5004/dwt.2022.28687

271 (2022) 65–73
September

Performance assessment of electrodeionization cell with different inter-membrane spacing and operating conditions

Aicha Lakehal[a,b,*], Kamel-Eddine Bouhidel[a]

[a]*Laboratory of Chemistry and Environmental Chemistry LCEE, Department of Chemistry, Faculty of Matter Sciences, University Hadj Lakhdar, Batna 1 05000, Algeria, emails: Lakehalaicha@yahoo.fr (A. Lakehal), ke.bouhidell@gmail.com (K.-E. Bouhidel)*
[b]*Faculty of Technology University, Batna 2, Algeria*

Received 2 February 2022; Accepted 1 July 2022

ABSTRACT

Electrodeionization (EDI) is a separation method that combines electrodialysis and ion-exchange. The continual electrical regeneration of the ion-exchange resin is the main advantage of this resulting hybrid process. The purpose of this study is to see how the inter-membrane spacing (resin bed thickness) affects EDI performance. For this purpose, resin beds thicknesses of 2, 4 and 6 mm were tested by varying operating conditions and the efficiency of the process was expressed in terms of mass transfer flux (J), current efficiency (C_e), removal efficiency (R), power consumption (P) and by the comparison of I–V curves. Our research indicated that the choice of thickness depends mainly on the electrical and hydrodynamic conditions used. Furthermore, an impressive empirical equation describing EDI efficiency as a function of flow rate and cell thickness was established.

Keywords: Electrodeionization; Electrodialysis; Ion-exchange; Bed thickness; Efficiency

1. Introduction

Electrodeionization (EDI) is a separation method combing ion-exchange (IE) with electrodialysis (ED). The resulting hybrid method on remove/received ions from water has gained a lot of attention.

Ion-exchange (IE) mixed bed has been used for decades in ultrapure water production. Much better efficiency is achieved in a sequential ion-exchange beds (cation-exchange bed, anion-exchange bed, mixed ion-exchange bed), especially in high water purity production (free of silica). In despite their high efficiency, the periodic chemical renewal of IE resins causes issues such as the use of toxic chemicals and the discharge of high-salinity wastewater [1,2].

Electrodialysis (ED) is a promising technology that is used in a number of industrial, laboratory, and recycling settings around the world [3–6]. Classical ED, according to its rule, is not applied to water demineralization – high energy demand and high resistance of the ED stack occur when improper parameters (too high current) are applied [7–12]. The EDI process has been suggested to eliminate these problems and to conciliate the advantages of two individual techniques. While EDI offers key benefits, it also has its drawbacks. The EDI system's performance might vary based on the feed water composition. It is, therefore, often used after reverse osmosis for the production of high purity water for industrial processes.

EDI can be considered, in principle, as an electrically regenerated ion-exchange column or an electrodialysis system with improved conductivity and selectivity due to the presence of ion-exchange particles in the dilute compartment.

A typical electrodeionization cell consists of alternating permselective anion- and cation-exchange membranes,

* Corresponding author.

ion-exchange resins (anion and cation-exchange resins) and a pair of electrodes (anode and cathode) at the ends of the ED stack (Fig. 1).

As the solution to be treated enters the EDI module, the charged ions are captured by the ion-exchange resins. On imposing direct electric field (voltage) across the cell, the EDI separation process is initiated. The cationic and anionic ions begin to move across the resin bed toward the appropriate electrode. Ion-selective membranes regulate this migration. Only negatively charged ions move through the anionic membrane, whereas positively charged ions are blocked. A cationic membrane does the exact opposite.

Thus, two types of chambers are created: one with a very low ionic concentration, known as a dilute chamber, and another with a high ionic concentration, known as a concentrate chamber. Ion-exchange resins are important to the EDI process because they increase ion transport and can also serve as a substrate for electrochemical reactions, including water dissociation into H^+ and OH^- ions. Since the produced hydrogen and hydroxyl ions electrochemically regenerate the ion-exchange resins without the use of chemicals, EDI can be considered an environmentally friendly process [13–20]. The basic principle of the EDI process is thoroughly summarized in the literature.

EDI has been used primarily in the generation of ultrapure water for energy, microelectronics, chemical, and pharmaceutical industries since its initial commercialization in 1987 [1,18–24]. Also, the EDI technique has received a great deal of attention in waste water treatment and chemical purification/recovery [21–23,25–31].

The equipment used for EDI studies contains a number of test cells of plate and frame design, spiral wound design, rectangular and cylindrical shape and a variety of sizes [27,32,33]. These cells consist of several chambers and with various ion-exchange resin compositions (mixed bed, layered bed and separate bed) [34–38]. The results of the operation can vary depending on the method of resin filling between the ion-exchange membranes. Other configurations using ion-exchange textile material instead of resins were also tested [39–41].

Several modifications of the original EDI stack design have been proposed to improve the efficiency of this technology [13,14,42,43]. However, the optimization of system design and operation conditions is still necessary and many process parameters are interesting to investigate and analyze for a better understanding and for better application of EDI.

The optimization of the EDI resin bed was and continues to be a significant challenge for the design. What is the most effective design? Thin or thick cells, Single or mixed bed. So far, very few works have been focused on this topic [44]. To our knowledge, the effect of the inter-membrane distance on the efficiency of the process by varying the operating parameters has not been studied. Therefore, our current research focuses on this optimization problem.

The experiments were carried out by an EDI cell having mixed bed configuration in the central compartment and the inter-membrane spacing effect on EDI performance was examined with resin bed thicknesses of 2, 4 and 6 mm under two different operating conditions.

2. Materials and methods

2.1. Chemicals and ion-exchange materials

The ion-exchange resins (IE) used in the dilute compartment were obtained from Merck (Germany). The physical and chemical characteristics are shown in Table 1.

The anion- and cation-exchange membranes used to separate compartments were Selemion AMV and CMV membranes (Asahi Glass, Japan). The properties are given in Table 2.

All experiments were carried out with the following chemicals (high-purity grade) from Merck (Germany): NaCl, Na_2HPO_4, NaH_2PO_4, and double-distilled water.

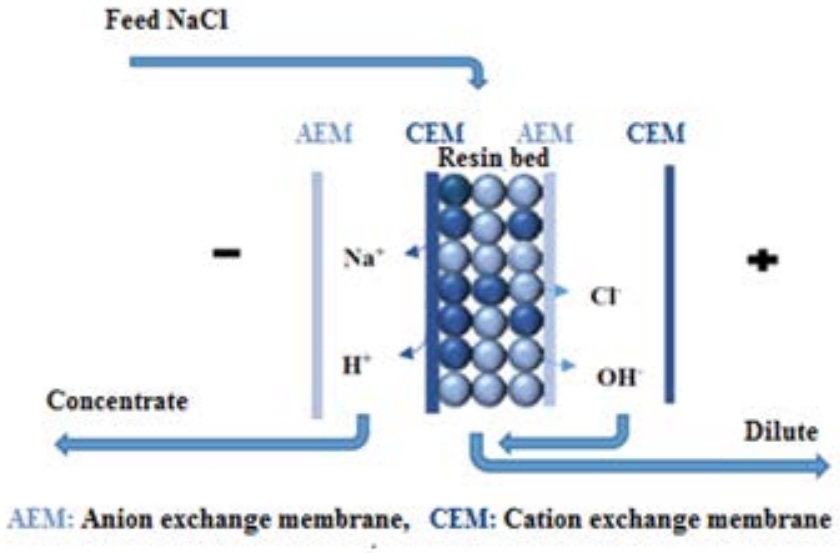

Fig. 1. Schematics of EDI process.

Table 1
Main characteristics of ion-exchange resin [10]

	Strongly acidic cation-exchange resin	Weakly basic anion-exchange resin
Type	Merck/Art.4765 (LAB)	Merck/Art. 4766 (LAB)
Ionic form as shipped	H^+	OH^-
Total exchange capacity, meq/g	4.5	5
Apparent volumic mass, g/mL	0.8	0.5
Water content, %	45–55	35–45
Granulometry, mesh (ASTM)	20–50 or 0.3–0.9 mm	20–50 or 0.3–0.9 mm

Table 2
Main characteristics of ion-exchange membrane [10]

	Cation-exchange membrane (CEM)	Anion-exchange membrane (AEM)
Type	Selemion CMV	Selemion AMV
Thickness, mm	0.15	0.14
Efficient area, cm^2	2.88	2.88
Ion-exchange capacity, meq/g	2.4	1.9
Resistance, Ω cm^2	2–3.5	2–3.5

2.2. Experimental procedures

For the EDI experiments, a four-electrode cell with three compartments was used. This cell was constructed of Plexiglas, inert material of great chemical and mechanical resistance.

The Selemion AMV anion-exchange and Selemion CMV cation-exchange membranes were used to separate the cell's anodic and cathodic compartments from the central compartment. The dilute compartment is located in the middle. It was filled with an intimate mixture of both cation-exchange resins and anion-exchange resins in a 1:1 ratio. This compartment is located between the two ion-selective membranes. The experiments were conducted with resin beds thicknesses (inter-membrane spacing) of 2, 4 and 6 mm. The effective membrane area is 2.88 cm^2. In the dilute compartment were placed two gold electrodes wires (φ = 0.6 mm) on both surfaces of the membrane and at both ends of the cell, ordinary commercial carbon electrodes were used as cathode and anode. For the I–V curve investigation, all four electrodes are connected to the Autolab PGSTAT30, allowing both automated current (or potential) scanning and simultaneous measurement of the potential difference (or current). A schematic view of the experimental set-up is depicted in Fig. 2.

The effect of inter-membrane spacing on salt removal in EDI device was demonstrated experimentally with resin bed thicknesses of 2, 4 and 6 mm under two different operating conditions. At the same voltage and the same flow rate, the experiments were conducted in the constant flow rate of 3 ml/min. For the same operating condition of electrical field and flow velocity, flow velocity of 20.8 cm/min was used and was kept equal in the three resin bed thicknesses.

The efficiency of the process was calculated in terms of mass transfer flux (J), removal efficiency (R), current efficiency (C_e), power consumption (P) and by the comparison of I–V curves.

The I–V curves (intensity of the current according to the transmembrane voltage) were obtained in potentiostatic mode using an Autolab PG STAT30 Instrument with scan rate of 50 mV s^{-1}.

The experiments of demineralization were performed in a constant potential mode of power supply.

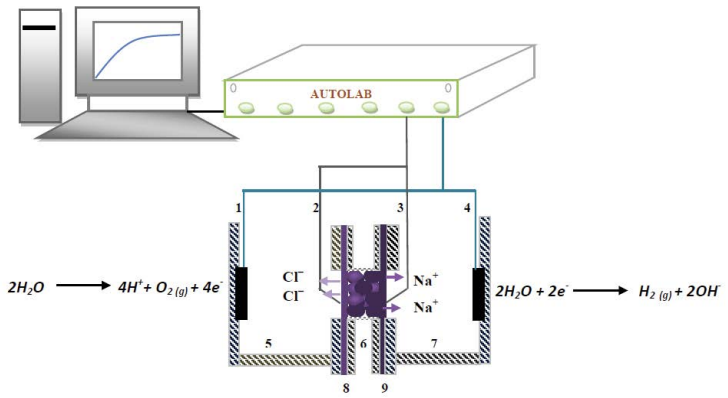

Fig. 2. Schematic description of the experimental cell and current-voltage measurements. (1) Working electrode, (2) sensor electrode, (3) reference electrode, (4) counter electrode, (5) anode compartment, (6) central compartment filled with ion-exchange resins, (7) cathode compartment, (8) anion-exchange membrane, (9) cation-exchange membrane.

The current intensity was recorded using a digital multimeter and the potential drop through the mixed bed was measured using the two gold electrodes wires. All experiments were carried out with 0.006 M solution of NaCl salt at room temperature. The central compartment is percolated by a sodium chloride solution from the feed tank. Samples (15 mL) were taken from the center compartment at regular time intervals for analysis. The solutions in both electrodes compartments were buffered by hydrogen/dihydrogen phosphate. The pH was maintained constant (near 7) during the run. This avoids H^+ and OH^- interference in the center compartment.

The pH and electrical conductivity of the treated solution were measured using a pH/Ion meter (pH M240, MeterLab) and a conductivity meter Tacussel, respectively.

The pH maintained nearly constant until polarization, at which point it began to change. The conductometry is used for measurements of NaCl concentration.

Because the ion-exchange resin alone can exchange ions without an electric field, the counter ions in the resins were replaced with sodium (cation-exchange) and chloride (anion-exchange) ions prior to the EDI operations. The feed solutions were used to equilibrate the ion-exchange membrane and ion-exchange resins. This phase was completed without the use of electricity.

2.3. Data analysis

The EDI process performance can be evaluated in terms of removal efficiency (R), flux (J), current efficiency (C_e) and power consumption (P).

The calculation of the removal efficiency (R) was carried out using the following formula:

$$R\% = \left(1 - \frac{C_f}{C_i}\right) \times 100 \quad (1)$$

The removed salt quantity (flux J) at a given voltage is:

$$J = Q\left(C_i - C_f\right) \quad (2)$$

The current efficiency (C_e) represents the ratio of the current that transfers salt to the total amount of applied current. The following equation was used to calculate C_e [36]:

$$C_e = Z \times F \times Q \times \frac{C_i - C_f}{I} \times 100 \quad (3)$$

Power consumption (P) in Wh eq^{-1} represents the amount of energy required to transport one gram equivalent of NaCl from dilute compartment to concentrate compartment. P has been calculated by the following equation [1]:

$$P = \int_0^t VI \frac{dt}{w} \quad (4)$$

where C_i and C_f represent the initial and final NaCl concentrations (mol L^{-1}), in dilute compartment, respectively; F is the Faraday constant (96,500 Ceq^{-1}); Q is the feed flow rate (L s^{-1}); I is the current (A); Z is the ion-charge; V is the applied potential (V) and w is the amount of salt (eq) removed.

3. Results and discussion

3.1. Current intensity

The current-voltage curves (intensity of the current according to the transmembrane voltage) measured in potentiostatic mode during continuous electrodeionization at the same voltage and the same flow rate are shown in Fig. 3a. Regardless of the cell's thickness, three main regimes appeared in the I–V relations, which are Ohmic, limiting, and overlimiting regimes.

Such regime diversification is due to the ion concentration polarization (ICP), which occurs as a result of variations in the transport numbers of ions in the solution and ion-exchange material (membranes and resins), as well as the need for electroneutrality. When ions pass through a permselective membrane or resin, dynamic changes of ion concentration occur near ion-exchange material

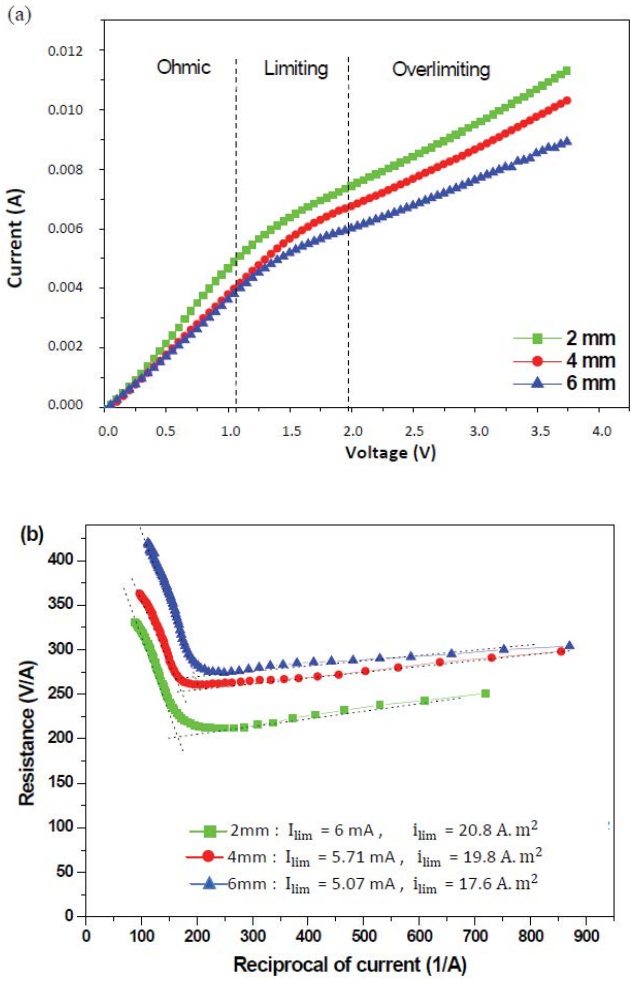

Fig. 3. Cell thickness effect on the current intensity at the same voltage and the same flow rate: (a) current transmembrane voltage curve and (b) limiting current determination curve (C_i = 0.006 mol/L; flow rate = 3 ml/min).

(membranes and resins), resulting in ion depletion zone towards one side of the material and in an enrichment of ions towards the other side. The voltage-current response was governed par the ion depletion zone of ICP.

- *Ohmic regime*: at relatively low voltage, negligible ion concentration polarization lets the voltage-current obeys Ohm's law with nearly constant electric resistance.
- Limiting regime where the curve (I–V) drew a non-linear region. When ion concentration polarization becomes important at a higher voltage, the development of the ion depletion zone induces an increase of electric resistance. The growth rate of the current is then slowed, and eventually exhibits saturation when the ion concentration becomes zero at the interface of the ion-exchange material and an electrolyte in ion depletion zone. The saturated current is known as a limiting current. In the present study, the limiting current (i_{lim}) was measured using the Cowan–Brown method, which relies on the relationship between electric resistance and the reciprocal value of the current.
- The intersection of two extrapolated sloping lines represents the limiting current (Fig. 3b).
- Overlimiting regime which was subsequently evolved as the current increased once more. We note that the overlimiting regime slope is smaller than that of the Ohmic regime, which is a common characteristic of the I–V curve in electrodialysis and this is different to that in the systems with bipolar membranes.

When the current intensities were compared, the corresponding cells present the following ascending order: EDI6 (6 mm) < EDI4 (4 mm) < EDI2 (2 mm). Significantly higher values are found in the thin cell. The greater the voltage applied, the greater the difference between the intensities of the current flowing through the different cells.

The values of the limiting current density appearing above a certain voltage threshold, were 20.8, 19.8 and 17.6 A m^{-2} for cell thickness of 2, 4 and 6 mm, respectively. The EDI system using the cell thickness of 6 mm showed the lowest i_{lim} compared with the other two cells.

The comparison will be even more clear and meaningful under the same experimental conditions of electrical field and flow velocity. Fig. 4 shows the reverse order.

The current intensity measured was appreciably larger in the thick cell (6 mm thick). Fig. 4 also shows that the current difference between different cell increases with an increase in electrical field.

The current flowing through the central compartment of an EDI cell is complicated since it is made up of two distinct phases: ion conducting resin and interstitial liquid. A low concentration solution is commonly used in an EDI system, as more current is expected to flow through the resin particles that are in contact with one another. In order for the resin to transport an ion and to maximize the overall deionization, there must be a continuous path of the appropriate type of ion-exchange resin for both anions and cations. From these results, we can see that an optimum inter-membrane resin distance can be identified, dependent on the operating conditions.

3.2. Mass transfer flux

At the same voltage and the same flow rate, the magnitude of mass transfer flux for the three resin bed thicknesses tested follows the order: EDI6 < EDI4 < EDI2. Significantly higher flux values are noted in the thin cell (2 mm) (Fig. 5a). The best performance of this cell is justified by:

- The distance to be covered by the ion is less, and the driving force is higher.
- At low thickness, the flow velocity, so Reynolds is higher, thus promoting solution-grain diffusion.

The evolution of the mass transfer flux within different cells under the same experimental conditions of electrical field and flow velocity is illustrated in Fig. 5b. The flux increases considerably with the increase in the thickness of the resin bed. The flux is proportional to both the electric field and the surface area of the resin. We expected a better flux with the thick cell. These observations are consistent with the current's variation.

3.3. Removal efficiency, current efficiency and power consumption

The removal efficiency (R), current efficiency (C_e) and power consumption (P) values are the crucial parameters of the electrodeionization process. For an effective electrodeionization process, the P value must be lower and the R and C_e values must be higher.

The effect of resin bed thickness on the removal efficiency at the same voltage and the same flow rate is illustrated in Figs. 6 and 7.

In Fig. 6, the removal efficiency R is plotted as a function of the applied voltage for the three resin bed thickness tested. It can be observed that R values increase with increasing voltage. This is due to the fact that the applied voltage was the main drain force for the electrodeionization process and that the velocity of ion migration was increasing from the central compartment to the concentrate compartments. Meanwhile, the current intensity

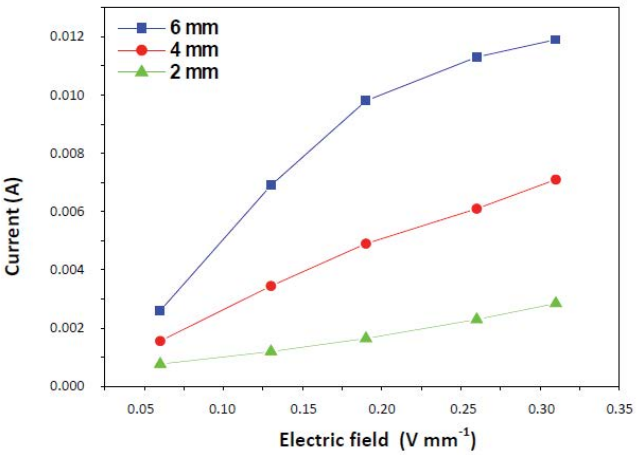

Fig. 4. Cell thickness effect on the current intensity at the same electrical field and the same flow velocity (C_i = 0.006 mol/L; flow velocity = 20.8 cm/min).

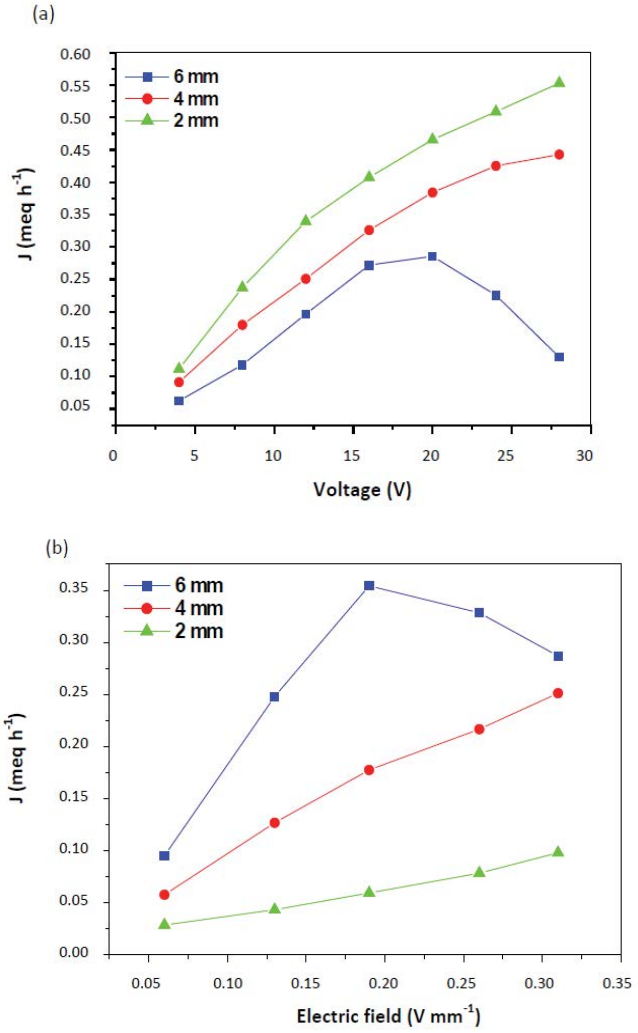

Fig. 5. Cell thickness effect on the mass transfer flux: (a) at the same voltage and the same flow rate and (b) at the same electrical field and the same flow velocity (C_i = 0.006 mol/L; flow rate = 3 ml/min; flow velocity = 20.8 cm/min).

increased with the increase in voltage. Moreover, a fall in the removal efficiency R was observed by increasing the thickness, notably at high voltage. It can be seen that the thin cell has the highest removal efficiency on all the range of potential considered. However, at high values of potential, this remarkable increase in R is limited due to the phenomenon of concentration polarization. It is now well known that a phenomenon such as the dissociation of water is increased in the contact areas of the ion-exchangers of opposite signs. This phenomenon is more important in the thick cell which decreases its efficiency.

Similarly, the experimental curves illustrating the variation in the removal efficiency as a function of flow rate confirm this result (Fig. 7a). For the three thicknesses examined, it can be seen that the efficiency of the process decreases rapidly with the increase in flow rate and the thin cell still has the best removal efficiency.

The experimental data points gave a reproducible linear curve in bi-logarithmic coordinates for the different

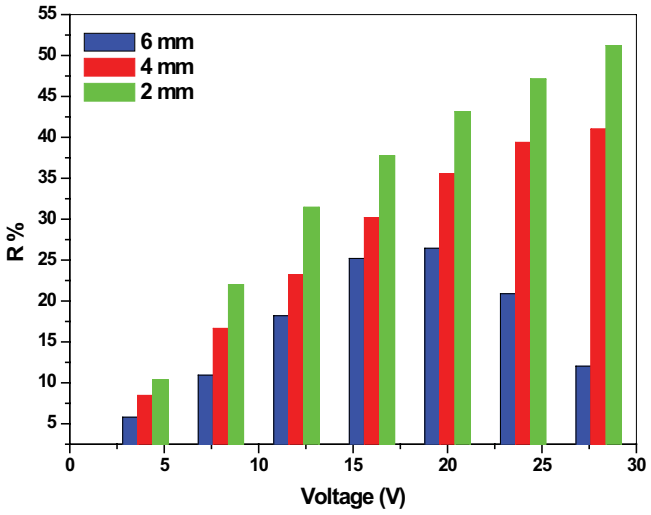

Fig. 6. Variation of the removal efficiency vs. the applied voltage for the three resin bed thickness (C_i = 0.006 mol/L; flow rate = 3 ml/min).

resin bed thicknesses examined (Fig. 7b). The corresponding equation has this simple form:

$$\log R = n \log Q + \log k \tag{5}$$

The slope of the line is n, and the intercept is log k.

The above equation may be expressed as:

$$R = kQ^n \tag{6}$$

The adjustment parameters of this equation for each thickness are presented in Table 3.

The parameter K is a constant dependent on thickness (K increases with decreasing thickness); while n is always close to –0.5. As a result, there is a well-defined relationship between removal efficiency and flow rate, as follows:

$$R = \frac{k}{\sqrt{Q}} \text{ or } R = \frac{K\sqrt{Q}}{Q} \tag{7}$$

It's a linear equation, as Freundlich isotherm, whatever the applied voltage.

Q reflects the residence time of an ion in the resin bed and $\sqrt{Q}$ reflects the agitation.

It is also possible to establish a linear relationship between the cell thickness and the reciprocal of the constant K (Fig. 7c):

$$\frac{1}{k} = \alpha + \beta x \tag{8}$$

where α and β are equal to 0.0216 and 0.0028 respectively.

The flux $J = Q\Delta C$ is then directly proportional to Q and inversely proportional to $\sqrt{Q}$.

This result contributes seriously to the best basic and design knowledge of the electrodeionization process.

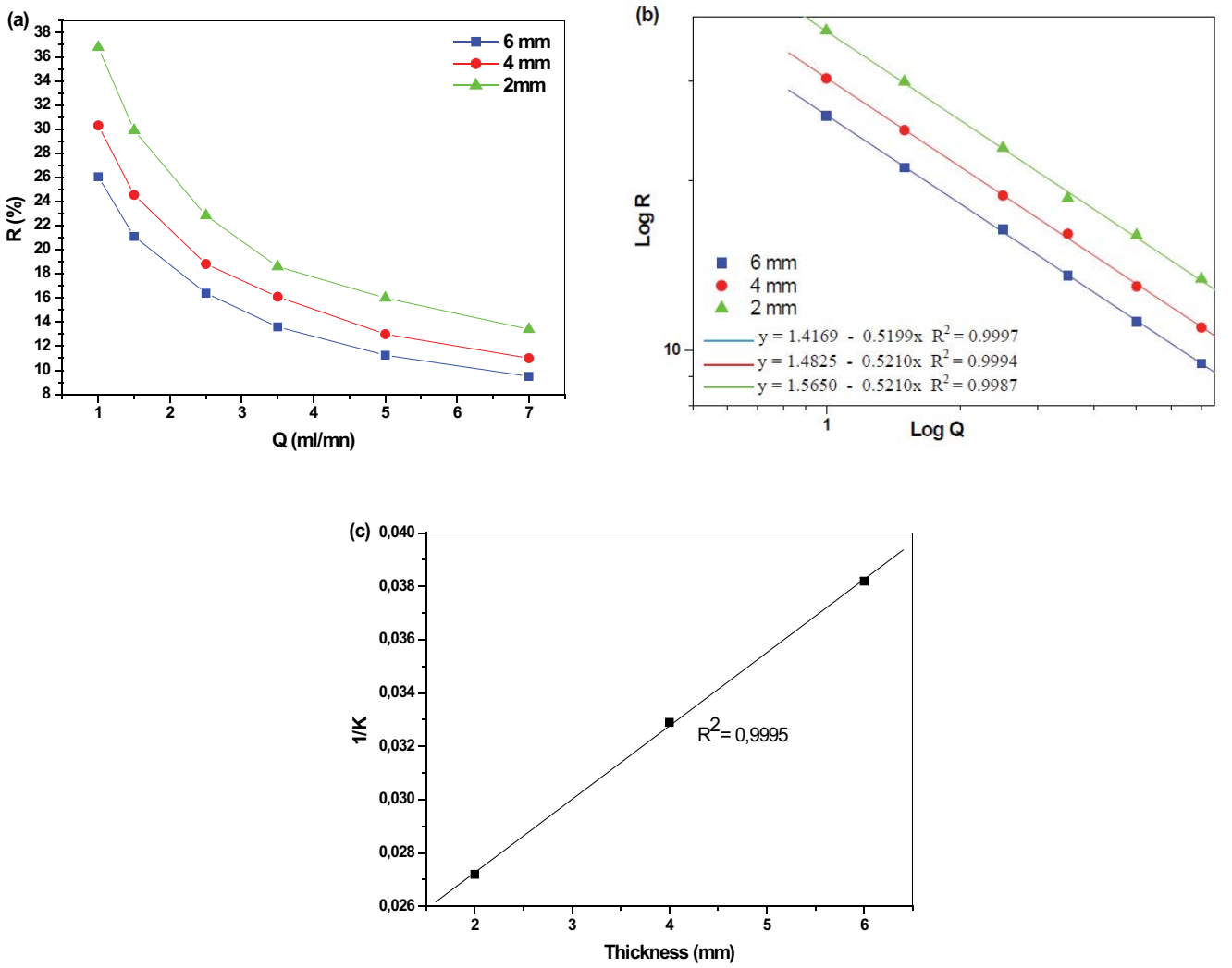

Fig. 7. Flow rate dependence of removal efficiency for three resin bed thickness. (a) Variation of the removal efficiency vs. flow rate. (b) Logarithmic scale representation of the removal efficiency evolution as a function of flow rate. (c) Variation of the ratio 1/*K* according to the resin bed thickness (C_i = 0.006 mol/L; voltage = 7 V).

Table 3
Parameters of R equation for different resin bed thickness

Resin bed thickness (mm)	6	4	2
n	–0.52	–0.52	–0.52
K	26.05	30.30	36.78

It offers several analogies with equations of hydrodynamics electrochemistry. An increase in Reynolds number decreases both the limiting layer thickness and the solution crossing time through the mixed bed.

Significant differences in the performance of the different cells were also observed by adjusting the operating parameters (electric field and flow velocity). The removal efficiency (Fig. 8) increases remarkably with the increase in thickness of the resin bed, especially at low fields where polarization phenomena are negligible. Under these identical operating conditions, the thin cell is characterized by a short distance to be travelled by the ion, which suggests

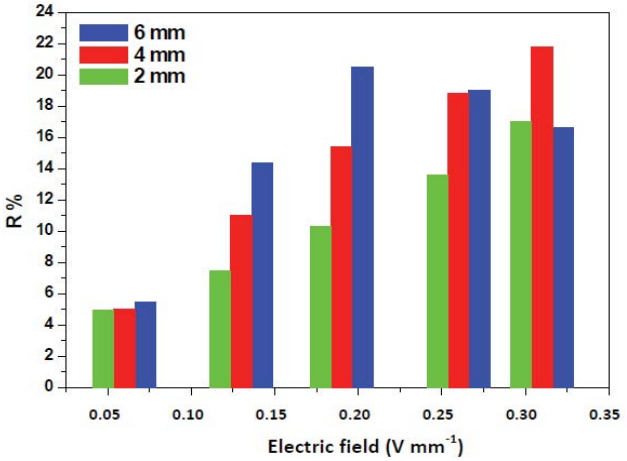

Fig. 8. Resin bed thickness effect on the removal efficiency at the same electrical field and the same flow velocity (C_i = 0.006 mol/L; flow velocity = 20.8 cm/min).

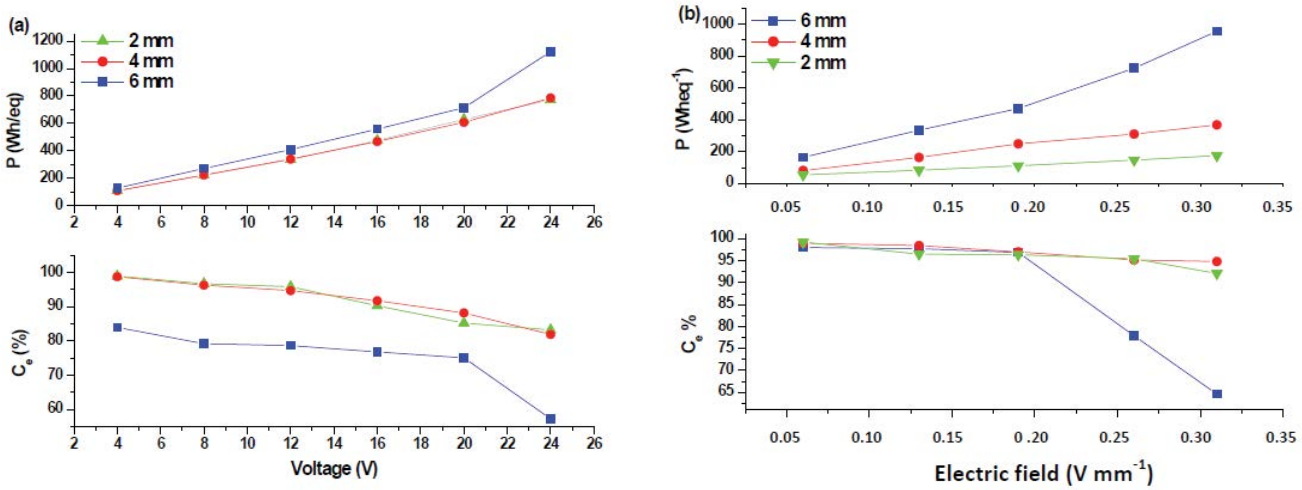

Fig. 9. Thickness dependence of current efficiency (C_e) and power consumption (P). (a) Tests performed at the same voltage and the same flow rate and (b) tests performed at the same electrical field and the same flow velocity (C_i = 0.006 mol/L; flow rate = 3 ml/min; flow velocity = 20.8 cm/min).

that it is the most efficient cell. However, the thick cell has a large exchange surface that outweighs the distance.

The performance of electrodeionization was also evaluated in terms of current efficiency (C_e) and power consumption (P).

At the same voltage and the same flow rate (Fig. 9a), it is observed that C_e decreased while P increased with an increase in the applied potential from 4 to 24 V for all cell examined. The C_e and P values of EDI2 are close to those of EDI4. The EDI6 has the highest power consumption and the lowest current efficiency mainly at high voltage, because the limiting current density (LCD) may be exceeded and water splitting will inevitably occur. This observation was also found in the same experimental conditions (Fig. 9b). Increasing electric field led to the declines of current efficiency and remarkable increases of power consumption in the thick cell. Also, it can be seen from Fig. 9b that the power consumption decreases with decreasing cell thickness.

The cells thickness of 2 and 4 mm show similar trends and the difference between their performances is not large.

4. Conclusions

The findings of the study revealed that the resin bed thickness (inter-membrane distance) has an important effect on the process efficiency and the extent of deionization can be modified by varying the operating conditions.

At the same voltage and the same flow rate, electric current, mass transfer flux, removal efficiency follow the order as EDI2 > EDI4 > EDI6. The current efficiency of all cells tested showed a downward trend, whereas the energy consumption showed an upward trend. The current efficiency follows the order as EDI6 < EDI4 ~ EDI2, and the order of energy consumption is EDI6 > EDI4 ~ EDI2.

At the same field and the same velocity, the electric current, mass transfer flux, removal efficiency follow the analogous order as EDI6 > EDI4 > EDI2. The power consumption decreases with decreasing cell thickness. At the high electric field P increased sharply for EDI6 cell, whereas it increased slowly for EDI4 and EDI2 and the order of current efficiency is EDI6 < EDI4 ~ EDI2. In conclusion, the smaller inter-membrane distance resulted in higher process efficiency at the same voltage and the same flow rate, while at the same field and the same velocity, the increase of inter-membrane distance led to better process efficiency, but high power consumption remained as a drawback. So the inter-membrane distance of 2–4 mm appears to allow the best results.

An important empirical equation describing the EDI characteristics (mass transfer flux and efficiency) as functions of flow rate and cell thickness was established. This equation provides valuable information and contributes to a better understanding of the EDI process.

References

[1] V. Bhadja, B.S. Makwana, S. Maiti, S. Sharma, U. Chatterjee, Comparative efficacy study of different types of ion-exchange membranes for production of ultrapure water via electrodeionization, Ind. Eng. Chem. Res., 54 (2015) 10974–10982.

[2] J. Hu, Z. Fang, X. Jiang, T. Li, X. Chen, Membrane-free electrodeionization using strong-type resins for high purity water production, Sep. Purif. Technol., 144 (2015) 90–96.

[3] S. Al-Amshawee, M.Y.B.M. Yunus, A.A.M. Azoddein, D.G. Hassell, I.H. Dakhil, H.A. Hasan, Electrodialysis desalination for water and wastewater: a review, Chem. Eng. J., 380 (2020) 122231, doi: 10.1016/j.cej.2019.122231.

[4] C.C.N. Kunrath, D.C. Patrocínio, M.A. Siqueira Rodrigues, T. Benvenuti, F.D.R. Amado, Electrodialysis reversal as an alternative treatment for producing drinking water from brackish river water: a case study in the dry season, northeastern Brazil, J. Environ. Chem. Eng., 8 (2020) 103719, doi: 10.1016/j.jece.2020.103719.

[5] C.S.L. dos Santos, M.H. Miranda Reis, V.L. Cardoso, M.M. de Resende, Electrodialysis for removal of chromium (VI) from effluent: analysis of concentrated solution saturation, J. Environ. Chem. Eng., 7 (2019) 103380, doi: 10.1016/j.jece.2019.103380.

[6] M. Ben Sik Ali, A. Mnif, B. Hamrouni, M. Dhahbi, Electrodialytic desalination of brackish water: effect of process parameters and water characteristics, Ionics (Kiel), 16 (2010) 621–629.

[7] C. Ahmed Basha, K. Ramanathan, R. Rajkumar, M. Mahalakshmi, P. Senthil Kumar, Management of chromium plating rinsewater using electrochemical ion-exchange, Ind. Eng. Chem. Res., 47 (2008) 2279–2286.
[8] K.-E. Bouhidel, A. Lakehal, Influence of voltage and flow rate on electrodeionization (EDI) process efficiency, Desalination, 193 (2006) 411–421.
[9] K.-E. Bouhidel, A. Lakehal, The prevention of the concentration polarization and the water dissociation in electrodeionization by an amphoteric salt NH_4CH_3COO, Desalination, 200 (2006) 627–628.
[10] A. Lakehal, K.-E. Bouhidel, Optimization of the electrodeionization process: comparison of different resin bed configurations, Desal. Water Treat., 86 (2017) 96–101.
[11] H. Strathmann, A. Grabowski, G. Eigenberger, Ion-exchange membranes in the chemical process industry, Ind. Eng. Chem. Res., 52 (2013) 10364–10379.
[12] M. Ben Sik Ali, A. Mnif, B. Hamrouni, Modelling of the limiting current density of an electrodialysis process by response surface methodology, Ionics (Kiel), 24 (2018) 617–628.
[13] J. Hu, Y. Chen, L. Zhu, Z. Qian, X. Chen, Production of high purity water using membrane-free electrodeionization with improved resin layer structure, Sep. Purif. Technol., 164 (2016) 89–96.
[14] Y. Liu, J. Wang, Y. Xu, B. Wu, A deep desalination and anti-scaling electrodeionization (EDI) process for high purity water preparation, Desalination, 468 (2019) 114075, doi: 10.1016/j.desal.2019.114075.
[15] B. Senthil Rathi, P. Senthil Kumar, Electrodeionization theory, mechanism and environmental applications. A review, Environ. Chem. Lett., 18 (2020) 1209–1227.
[16] X. Shen, Z. Fang, J. Hu, X. Chen, Membrane-free electrodeionization for purification of wastewater containing low concentration of nickel ions, Chem. Eng. J., 280 (2015) 711–719.
[17] W. Su, R. Pan, Y. Xiao, X. Chen, Membrane-free electrodeionization for high purity water production, Desalination, 329 (2013) 86–92.
[18] X. Sun, H. Lu, J. Wang, Brackish water desalination using electrodeionization reversal, Chem. Eng. Process. Process Intensif., 104 (2016) 262–270.
[19] J.-H. Song, K.-H. Yeon, S.-H. Moon, Effect of current density on ionic transport and water dissociation phenomena in a continuous electrodeionization (CEDI), J. Membr. Sci., 291 (2007) 165–171.
[20] C. Femina Carolin, P. Senthil Kumar, A. Saravanan, G. Janet Joshiba, Mu. Naushad, Efficient techniques for the removal of toxic heavy metals from aquatic environment: a review, J. Environ. Chem. Eng., 5 (2017) 2782–2799.
[21] L. Alvarado, A. Chen, Electrodeionization: principles, strategies and applications, Electrochim. Acta, 132 (2014) 583–597.
[22] Ö. Arar, Ü. Yüksel, N. Kabay, M. Yüksel, Various applications of electrodeionization (EDI) method for water treatment—a short review, Desalination, 342 (2014) 16–22.
[23] S. Kumar, M. Bhushan, M. Manohar, B.S. Makwana, V.K. Shahi, In-sight studies on concentration polarization and water splitting during electro-deionization for rapid production of ultrapure water (@18.2 MΩ cm) with improved efficiency, J. Membr. Sci., 589 (2019) 117248, doi: 10.1016/j.memsci.2019.117248.
[24] P. Rychen, J. Leet, The use of EDI in treating semiconductor grade water, Ultrapure Water, 17 (2000) 36–40.
[25] L. Alvarado, I.R. Torres, A. Chen, Integration of ion-exchange and electrodeionization as a new approach for the continuous treatment of hexavalent chromium wastewater, Sep. Purif. Technol., 105 (2013) 55–62.
[26] K. GracePavithra, V. Jaikumar, P. Senthil Kumar, P.S. Sundar-Rajan, A review on cleaner strategies for chromium industrial wastewater: present research and future perspective, J. Cleaner Prod., 228 (2019) 580–593.
[27] A. Mahmoud, A.F.A. Hoadley, An evaluation of a hybrid ion-exchange electrodialysis process in the recovery of heavy metals from simulated dilute industrial wastewater, Water Res., 46 (2012) 3364–3376.
[28] Z. Zhang, D. Liba, L. Alvarado, A. Chen, Separation and recovery of Cr(III) and Cr(VI) using electrodeionization as an efficient approach, Sep. Purif. Technol., 137 (2014) 86–93.
[29] H.R. Taghdirian, A. Moheb, M. Mehdipourghazi, Selective separation of Ni(II)/Co(II) ions from dilute aqueous solutions using continuous electrodeionization in the presence of EDTA, J. Membr. Sci., 362 (2010) 68–75.
[30] F. Sun, G. Wei, H. Du, C. Yang, Performance of continuous electrodeionization technique during the purification of the nonaqueous organic solvent N,N-dimethylformamide, Sep. Purif. Technol., 199 (2018) 242–250.
[31] G.M. Zeng, J. Ye, M. Yan, Application of electrodeionization process for bioproduct recovery and CO_2 capture and storage, Curr. Org. Chem., 20 (2016) 2790–2798.
[32] J. Wood, J. Gifford, J. Arba, M. Shaw, Production of ultrapure water by continuous electrodeionization, Desalination, 250 (2010) 973–976.
[33] F. Liu, G. Zhang, H. Zhang, J. Mo, Performance evaluation of electrodeionization process based on ionic equilibrium with plate and frame modules, Desalination, 221 (2008) 425–432.
[34] S. Thate, N. Specogna, G. Eigenberger, A comparison of different EDI concepts used for the production of high-purity water, Ultrapure Water, 16 (1999) 42–56.
[35] K.-H. Yeon, J.-H. Song, S.-H. Moon, A study on stack configuration of continuous electrodeionization for removal of heavy metal ions from the primary coolant of a nuclear power plant, Water Res., 38 (2004) 1911–1921.
[36] Ö. Arar, Ü. Yüksel, N. Kabay, M. Yüksel, Demineralization of geothermal water reverse osmosis (RO) permeate by electrodeionization (EDI) with layered bed configuration, Desalination, 317 (2013) 48–54.
[37] J. Lu, X.-Y. Ma, Y.-X. Wang, Numerical simulation of the electrodeionization (EDI) process with layered resin bed for deeply separating salt ions, Desal. Water Treat., 57 (2016) 10546–10559.
[38] S.-Y. Pan, S.W. Snyder, Y.J. Lin, P.-C. Chiang, Electrokinetic desalination of brackish water and associated challenges in the water and energy nexus, Environ. Sci. Water Res. Technol., 4 (2018) 613–638.
[39] E. Dejean, J. Sandeaux, R. Sandeaux, C. Gavach, Water demineralization by electrodeionization with ion-exchange textiles. comparison with conventional electrodialysis, Sep. Sci. Technol., 33 (1998) 801–818.
[40] J.-H. Song, K.-H. Yeon, S.-H. Moon, Transport characteristics of Co^{2+} through an ion-exchange textile in a continuous electrodeionization (CEDI) system under electro-regeneration, Sep. Sci. Technol., 39 (2004) 3601–3619.
[41] M.B.C. Elleuch, M. Ben Amor, G. Pourcelly, Phosphoric acid purification by a membrane process: electrodeionization on ion-exchange textiles, Sep. Purif. Technol., 51 (2006) 285–290.
[42] K. Dermentzis, Removal of nickel from electroplating rinse waters using electrostatic shielding electrodialysis/electrodeionization, J. Hazard. Mater., 173 (2010) 647–652.
[43] X.-Y. Zheng, S.-Y. Pan, P.-C. Tseng, H.-L. Zheng, P.-C. Chiang, Optimization of resin wafer electrodeionization for brackish water desalination, Sep. Purif. Technol., 194 (2018) 346–354.
[44] J.H. Wood, G.C. Ganzi, P.A. Springthorpe, Continuous Electrodeionization: Module Design Considerations for the Production of High-Purity Water, Ion-Exchange at the Millennium, Eds. J.A. 2000.